ELSEVIER

Polymer 41 (2000) 1429–1439

polymer

Miscibility, melting and crystallization behavior of two bacterial polyester/poly(epichlorohydrin-*co*-ethylene oxide) blend systems

L.L. Zhang, S.H. Goh*, S.Y. Lee, G.R. Hee

Department of Chemistry, National University of Singapore, Singapore 119260, Republic of Singapore

Received 2 October 1998; received in revised form 5 April 1999; accepted 15 April 1999

Abstract

The miscibility, melting and crystallization behavior of two bacterial polyester/poly(epichlorohydrin-*co*-ethylene oxide) (PECH–EO) blend systems was studied. PECH–EO containing 48 mol% of epichlorohydrin is miscible with poly(3-hydroxybutyrate) (PHB) and with poly(3-hydroxybutyrate-*co*-3-hydroxyvalerate) (PHBV) containing 14 mol% hydroxyvalerate. Both blend systems are characterized by the existence of a single glass transition temperature (T_g) and a depression of the equilibrium melting temperature of PHB or PHBV in each blend. The T_g-composition dependence of the blends can be described by the Kwei equation. The interaction parameters obtained from melting point depression analysis are −0.089 and −0.075 for PHB/PECH–EO and PHBV/PECH–EO blends, respectively. The melting and cold crystallization behavior of PHB and PHBV during DSC heating runs is markedly affected by the addition of PECH–EO. During the non-isothermal crystallization process, the cold crystallization temperature (T_{cc}) of PHB first shows a slight decrease with increasing PECH–EO content from 0 to 50 wt.%, and then a significant increase with further increase of PECH–EO content to 90 wt.% in PHB/PECH–EO blends. For PHBV/PECH–EO blends, the T_{cc} of PHBV increases with increasing PECH–EO content in the whole composition range studied during the process. For samples after cold crystallization, the phase crystallinity of PHB remains constant, while that of PHBV decreases significantly with increasing PECH–EO content. Under isothermal condition, the radial growth rates of bacterial polyester spherulites in the blends are lower than that of pure bacterial polyester samples at higher crystallization temperatures. Spherulitic growth kinetics is analyzed using the Lauritzen–Hoffman model, and the kinetic parameters are determined. Nucleation constant decreases with increasing PECH–EO content in both PHB/PECH–EO and PHBV/PECH–EO blends.

Keywords: Bacterial polyesters; Poly(epichlorohydrin-*co*-ethylene oxide); Miscibility

1. Introduction

During the past decade, much attention has been paid to the production, physical properties, modification and utilization of bacterial polyesters owing to their potential applications as environment-friendly materials [1–4]. Bacterial polyesters fit perfectly well in the ecosystem due to their natural origin and biodegradability. They are produced via bacterial fermentation and can be completely degraded to carbon dioxide and water through bacterial action under various environmental conditions [5–8]. So far, poly(3-hydroxybutyrate) (PHB) and poly(3-hydroxybutyrate-*co*-3-hydroxyvalerate) (PHBV), a statistically random copolymer of 3-hydroxybutyrate (3HB) and 3-hydroxyvalerate (3HV), are the most well known members of the bacterial polyester family and have been commercially available under the trade name Biopol since the early 1980s [9].

However, both PHB and PHBV suffer from some disadvantages, such as relatively high cost of production and limited processing temperature ranges as compared to conventional, non-biodegradable thermoplastics with comparable physical properties such as polyethylene and polypropylene [10,11]. These drawbacks have hampered the utilization of PHB and PHBV as common plastics. Polymer blending is an accessible approach to widen the applications of bacterial polyesters [12,13]. Blending PHB and PHBV with other polymers may offer opportunities to extend and exploit their many useful and interesting properties, to modify the undesirable properties, and to lower cost.

There have been many studies on miscible blends containing PHB or PHBV. For example, PHB is miscible with poly(ethylene oxide) [14], poly(vinylidene chloride-*co*-acrylonitrile) [15] and poly(*p*-vinylphenol) (PVPh) [16]. It was recently reported that PHBV15 (15 mol% 3HV content)/PVPh blends are also miscible [17]. Of much interest are polymer blends of PHB and PHBV with various rubbery components, which may impart toughness

* Corresponding author. Fax: +65-7791691.
E-mail address: chmgohsh@nus.edu.sg (S.H. Goh)

0032-3861/00/$ - see front matter
PII: S0032-3861(99)00320-1

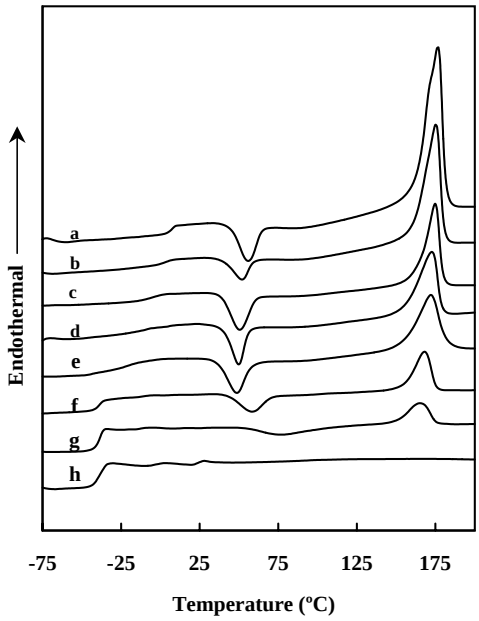

Fig. 1. DSC curves of PHB/PECH–EO blends after quenching from 200°C: (a) PHB; (b) 90/10; (c) 75/25; (d) 65/35; (e) 50/50; (f) 25/75; (g) 10/90 and (h) PECH–EO.

to bacterial polyester-based materials [18–26]. Some of the blends, such as PHB/ethylene–propylene rubber [18,19], PHB/ethylene–vinyl acetate copolymer (EVA) (containing 70 wt.% vinyl acetate) [20] and PHBV15/EVA (containing 28 mol% vinyl acetate) blends [21] are immiscible, and the ultimate toughness of the blends is markedly related to the particle size of the dispersed phase [19]. Miscible bacterial polyester/rubber blend systems are desirable for modifying PHB and PHBV. So far, only a few bacterial polyester/rubber blends are found to be miscible including PHB/poly(vinyl acetate) (PVAc) [18], PHBV9/PVAc [22], PHB/EVA (containing 85 wt.% vinyl acetate) [20] and PHB/poly(epichlorohydrin) (PECH) [23]. The miscibility, crystallization and biodegradation of PHB/PECH blends have been investigated in detail [23–26]. It has been demonstrated that the PECH molecules are dispersed at a molecular level in the interfibrillar zones.

Poly(epichlorohydrin-*co*-ethylene oxide) (PECH–EO) is a commercially available rubber with low glass transition temperature and hydrophilicity. In this paper, we focus on the miscibility, melting and crystallization behavior of PHB/PECH–EO and PHBV/PECH–EO blends.

2. Experimental

2.1. Materials

Bacterial PHB and PHBV (14 mol% 3HV content) were obtained from Aldrich. PHB was first dissolved in chloroform, filtered to remove cell wall residues, and then precipitated into methanol. The precipitate was filtered and dried at 60°C in vacuo. Its weight- and number-average molecular weights (M_w and M_n) are 2.3×10^5 and 8.7×10^4 g mol^{-1}, respectively, as determined by gel permeation chromatography with chloroform as the eluent. The M_w and M_n of PHBV are 4.54×10^5 and 1.53×10^5 g mol^{-1}, respectively. PECH–EO (66 wt.% or 48 mol% epichlorohydrin unit, density = 1.32 g cm^{-3}) was obtained from Aldrich. Its M_w and M_n are 4.4×10^5 and 9.6×10^4 g mol^{-1}, respectively.

2.2. Preparation of blends

Binary blends of PHB/PECH–EO and PHBV/PECH–EO of varying compositions were prepared by casting from 1% (w/v) chloroform solutions. The solvent was allowed to evaporate slowly at room temperature over night, followed by drying in vacuo at 40°C for 48 h and then at 70°C for 48 h.

2.3. Differential scanning calorimetry (DSC) measurements

DSC measurements were conducted on a TA Instruments 2920 differential scanning calorimeter. The instrument was calibrated with an indium standard and a nitrogen atmosphere was used throughout. All measurements were performed at a scanning rate of 20°C min^{-1}.

Cast samples were first heated from −100 to 200°C for PHB blends and to 180°C for PHBV blends. The samples were kept at 180 or 200°C for 1 min and then rapidly quenched by liquid nitrogen to −100°C (quenched samples). The quenched samples were then scanned to 200°C (180°C for PHBV blends). The glass transition temperatures (T_gs), melting temperatures (T_ms), enthalpies of fusion (ΔH_fs), cold crystallization temperatures (T_{cc}s) and enthalpies of cold crystallization (ΔH_{cc}s) were obtained from the corresponding transitions in the DSC curves. The T_m and T_{cc} were taken as the peak values of the respective endotherm and exotherm in the DSC curves. The T_g was taken as the midpoint of the specific heat increment. All results were based on the second heating run unless stated otherwise.

The equilibrium melting temperatures of PHB and PHBV in pure samples and the blends were obtained by heating the samples to above melting temperatures after isothermal crystallization at different crystallization temperatures according to the procedure of Pearce et al. [27].

2.4. Polarizing optical microscopy

The growths of PHB and PHBV spherulites in pure samples and in the blends were observed with an Olympus BH2-UMA polarizing optical microscope, equipped with a Leitz Wetzlar hot stage and an Olympus exposure control unit. Sample sandwiched between two thin glass slides was melted for 1 min on a hot-plate preheated to 200°C for PHB/PECH–EO blends or 180°C for PHBV/PECH–EO blends. It was then quickly transferred onto the hot stage of the microscope which was maintained at a desired temperature (T_c).

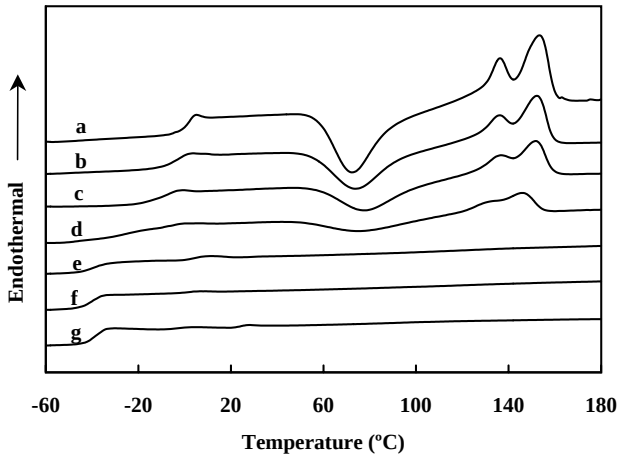

Fig. 2. DSC curves of PHBV/PECH–EO blends after quenching from 180°C: (a) PHBV; (b) 90/10; (c) 75/25; (d) 50/50; (e) 25/75; (f) 10/90 and (g) PECH–EO.

The sample was allowed to crystallize isothermally under crossed polars. The radial growth rate (G) of the spherulites was measured by photographing the spherulites as a function of time during isothermal crystallization. For all samples, G was calculated at different T_cs as $G = dR/dt$ (R is the spherulite radius).

3. Results and discussion

3.1. Miscibility of blends

Figs. 1 and 2 show the DSC curves of quenched samples of PHB/PECH–EO and PHBV/PECH–EO blends. Only one glass transition was found for each blend during DSC heating run. As shown in Figs. 3 and 4, the T_gs of the blends are composition-dependent and intermediate between those of the component polymers, indicating that both

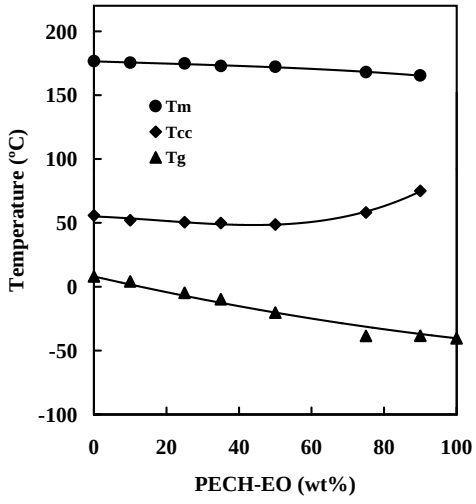

Fig. 3. Phase diagram of PHB/PECH–EO blends. T_g-composition curve was drawn using the Kwei equation $k = 1.0$, $q = -16.3$.

PHB/PECH–EO and PHBV/PECH–EO blends are miscible. The T_g-composition curve of a miscible blend system can be described by the Kwei equation [28].

$$T_g = \frac{w_1 T_{g1} + k w_2 T_{g2}}{w_1 + k w_2} + q w_1 w_2 \quad (1)$$

where T_g, T_{g1}, T_{g2} are the glass transition temperatures of the blend, polymer 1 and polymer 2, respectively, w_1 and w_2 are the weight fractions of polymer 1 and polymer 2, and k and q are fitting constants. The dependence of T_g on the composition of PHB/PECH–EO blends as shown in Fig. 3 can be well described by the Kwei equation using $k = 1.0$ and $q = -16.3$. Similarly, the T_g-composition curve of PHBV/PECH–EO blends as shown in Fig. 4 can also be fitted by the Kwei equation using $k = 1.05$ and $q = -15.1$.

Based on the Flory–Huggins theory [29], the free energy of mixing (ΔG_m) of two polymers is expressed by

$$\frac{\Delta G_m}{RT} = \frac{\phi_1}{N_1} \ln \phi_1 + \frac{\phi_2}{N_2} \ln \phi_2 + \chi_{12} \phi_1 \phi_2 \quad (2)$$

where χ_{12} denotes the Flory–Huggins interaction parameter of the two polymers 1 and 2 with volume fractions ϕ_1 and ϕ_2, and degrees of polymerization N_1 and N_2, respectively. A critical value of interaction parameter, χ_{crit}, which sets the upper limit for miscibility across the entire composition range is

$$\chi_{crit} = \frac{1}{2}\left(\frac{1}{\sqrt{N_1}} + \frac{1}{\sqrt{N_2}}\right)^2. \quad (3)$$

Miscibility occurs when $\chi_{12} < \chi_{crit}$. Since PECH–EO is a copolymer, the interaction parameter χ_{12} between PHB and PECH–EO, $\chi_{PHB/PECH–EO}$, is related to three segmental interaction parameters by the expression [30,31]

$$\chi_{PHB/PECH–EO} = y\chi_{PHB/PECH} + (1-y)\chi_{PHB/PEO} - y(1-y)\chi_{PECH/PEO} \quad (4)$$

where y is volume fraction of epichlorohydrin units in the PECH–EO copolymer.

The three binary blend systems, PHB/PECH [23], PHB/PEO [14] and PECH/PEO [32] are all miscible. Thus, the three segmental interaction parameters in Eq. (4) are all negative. According to Eq. (4), it is possible that $\chi_{PHB/PECH–EO}$ can be positive if $\chi_{PECH/PEO}$ is sufficiently negative such that

$$|\chi_{PECH/PEO}|^{1/2} > |\chi_{PHB/PECH}|^{1/2} + |\chi_{PHB/PEO}|^{1/2}. \quad (5)$$

$\chi_{PHB/PECH}$ and $\chi_{PHB/PEO}$ are -0.068 and -0.096, respectively [14,23]. The interaction energy density (B) for PECH/PEO blends is -3.93 J cm^{-3} [32]. Since $\chi_{12} = BV_1/RT_m^0$, $\chi_{PECH/PEO}$ is calculated to be -0.092 using the equilibrium melting point (T_m^0) of 349 K for PEO [32] and the molar volume (V_1) of 68.03 cm^3 mol^{-1} for PECH [33]. It is then found that Eq. (5) is not satisfied and therefore the so-called "immiscibility window" does not exist for the PHB/PECH–EO blend

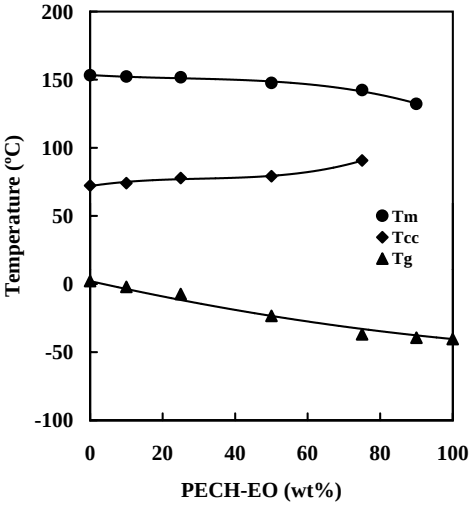

Fig. 4. Phase diagram of PHBV/PECH–EO blends. T_g-composition curve was drawn using the Kwei equation $k = 1.05$, $q = -15.1$.

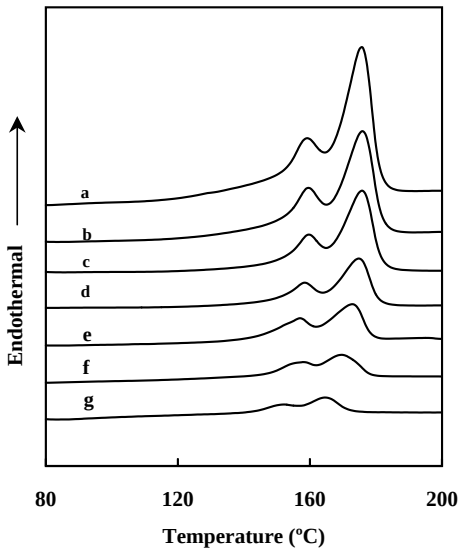

Fig. 5. DSC curves of PHB/PECH–EO cast blends: (a) PHB; (b) 90/10; (c) 75/25; (d) 65/35; (e) 50/50; (f) 25/75 and (g) 10/90.

system. In other words, PHB is expected to be miscible with PECH–EO at all copolymer composition ranges. On the other hand, $\chi_{PHBV/PECH-EO}$ is related to four intermolecular and two intramolecular segmental interaction parameters. Since not all the segmental interaction parameters are known, the miscibility of this blend system cannot be predicted.

3.2. Melting behavior

As shown in Fig. 1, the quenched samples of plain PHB and PHB/PECH–EO blends show only one melting peak of the PHB phase during DSC heating run. The apparent T_m of PHB decreases slightly with increasing PECH–EO content from 174°C for pure PHB to 164°C for the 10/90 blend (Fig. 3). For a miscible blend, thermodynamic factor can cause a marked depression of the equilibrium melting temperature. The apparent T_m of the blends is thus affected by both thermodynamic and morphological effects. The enthalpy of fusion (ΔH_f) of PHB/PECH–EO blend decreases regularly with increasing PECH–EO content for quenched samples after cold crystallization (Table 1). The thermodynamic melting enthalpy (ΔH_f^0) of a completely crystalline PHB is 146 J g^{-1} [34]. The crystallinity of the PHB phase in the blends, *Cr*, is calculated using the following equation:

$$Cr = \frac{\Delta H_f}{w_2 \Delta H_f^0} \times 100\% \quad (6)$$

where w_2 is the weight fraction of crystalline component in the blend. It can be concluded that *Cr* of PHB is almost constant when the PECH–EO content increases from 0 to 90 wt.% (Table 1).

During DSC heating run, the cast samples of PHB/PECH–EO blends show two separate endothermic peaks (Fig. 5) attributed to the occurrence of melting, recrystallization and remelting in the melting region [35–37]. The low-temperature peak located at about 167°C for pure PHB is associated with the as-formed crystals, while the high-temperature peak located at about 174°C for pure PHB is associated with the melting of the crystals formed from the recrystallization process during the DSC heating run. With increasing PECH–EO content, the peak temperatures of the two endotherms decrease. The ΔH_f of the cast sample of PHB/PECH–EO blend is larger than that of the corresponding quenched blend of the same blend

Table 1
Enthalpies and phase crystallinity of PHB in PHB/PECH–EO blends

Composition	Cast samples		Quenched samples		
	ΔH_f (J g^{-1})	*Cr* (%)	ΔH_f (J g^{-1})	$-\Delta H_{cc}$ (J g^{-1})	*Cr* (%)
100/0	88.9	60.9	79.2	15.1	54.3
90/10	80.0	60.9	70.2	10.6	53.4
75/25	66.1	60.4	60.3	23.5	55.1
65/35	57.4	60.5	51.0	20.8	53.8
50/50	44.6	61.1	38.6	17.0	52.9
25/75	22.2	60.8	19.6	11.4	53.6
10/90	8.8	60.4	7.7	4.2	52.5

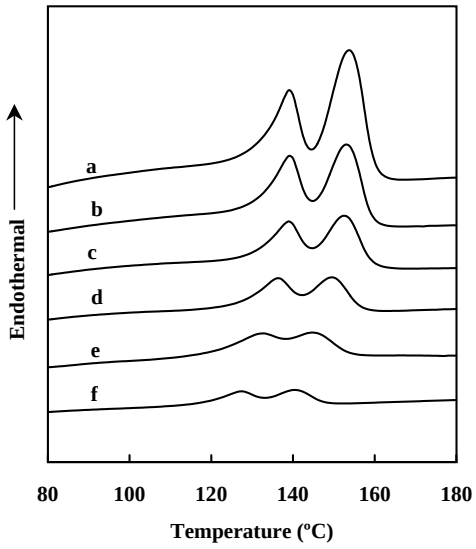

Fig. 6. DSC curves of PHBV/PECH–EO cast blends: (a) PHBV; (b) 90/10; (c) 75/25; (d) 50/50; (e) 25/75 and (f) 10/90.

composition as shown in Table 1. It also decreases linearly with increasing PECH–EO content, and the phase crystallinity of PHB remains constant in the cast samples.

For the PHBV/PECH–EO blends, it is noted that both the quenched and the cast samples of the blends show two separate endothermic peaks during the DSC heating runs (Figs. 2 and 6). With increasing PECH–EO content, the relative height of the first peak increases, while that of the second peak decreases, indicating a lower tendency of reorganization of original crystal in the blends. Both melting points of PHBV in the blends decrease with increasing PECH–EO content. With increasing PECH–EO content to 90 wt.%, the higher T_m decreases from 153 to 142°C for the quenched samples, and from 154 to 140°C for the cast ones; the lower T_m decreases from 136 to 126°C, and from 139 to 127°C, for the quenched and cast samples, respectively.

The ΔH_f of PHBV/PECH–EO blend decreases with increasing PECH–EO content (Table 2). The crystallinity of PHBV phase in the blends can also be calculated from Eq. (6). A value of 109 J g^{-1} for PHBV containing 10 mol% 3HV units [38] is used as an approximate value for PHBV used in this study. From Table 2, it can be concluded that *Cr* is lowered from 37 to 0.8% for the quenched samples when the PECH–EO content increases from 0 to 90 wt.%. For the cast samples, the ΔH_f of the blend is larger than that of the corresponding quenched blend of the same composition and it decreases with increasing PECH–EO content. The *Cr* of PHBV shows a slight decrease in the cast samples (Table 2).

3.3. Depression of equilibrium melting points

Figs. 7 and 8 show linear relationships between T_ms and crystallization temperatures (T_cs) in isothermal crystallization study for both blend systems. The equilibrium melting points (T_m^0s) of PHB and PHBV are determined by extrapolation to the lines of $T_m = T_c$ according to the Hoffman–Weeks equation [39]:

$$T_m = \frac{1}{\gamma} T_c + \left(1 - \frac{1}{\gamma}\right) T_m^0 \tag{7}$$

where γ is the ratio of the initial to the final lamellar thickness. The value of $1/\gamma$ is between 0 ($T_m = T_m^0$ for all T_c, in the case of most stable crystal) to 1 ($T_m = T_c$ in the case of inherently unstable crystal). The value of $1/\gamma$ is 0.1413 for pure PHB, and 0.1019, 0.1382 and 0.2048 for the blends containing 10, 25 and 50 wt.% PECH–EO, respectively. It is noted that PHB crystal in the 90/10 blend is more stable than that of pure PHB. The slopes of lines of T_m vs. T_c for the PHBV/PECH–EO blend system in Fig. 8 are close to each other. The value of $1/\gamma$ is about 0.35 which is almost independent of blend composition. As compared with PHB crystals, PHBV crystals are less stable.

Apart from the single T_g, the depression of the equilibrium melting point of the crystalline polymer is also an important characteristic demonstrating the miscibility of a semicrystalline/amorphous polymer blend system. As shown in Figs. 7 and 8, the equilibrium melting points of PHB and PHBV in the blends are depressed. It has been well established that such a depression is related to the interaction parameter χ_{12} between the two polymers as expressed by the Nishi–Wang equation [40]:

$$-\left[\frac{\Delta H^0 V_1}{R V_2}\left(\frac{1}{T_{mb}^0} - \frac{1}{T_m^0}\right) + \frac{\ln \phi_2}{N_2} + \left(\frac{1}{N_2} - \frac{1}{N_1}\right)\phi_1\right] = \beta = \chi_{12}\phi_1^2 \tag{8}$$

Table 2
Enthalpies and phase crystallinity of PHBV in PHBV/PECH–EO blends

Composition	Cast samples		Quenched samples		
	ΔH_f (J g^{-1})	*Cr* (%)	ΔH_f (J g^{-1})	$-\Delta H_{cc}$ (J g^{-1})	*Cr* (%)
100/0	41.4	38.0	40.3	40.3	37.0
90/10	37.7	38.5	37.1	36.1	37.8
75/25	30.2	36.9	28.1	27.9	34.4
50/50	19.8	36.3	16.4	15.5	30.1
25/75	9.7	35.6	0.8	0.4	2.8
10/90	3.9	35.5	0.1	0	0.8

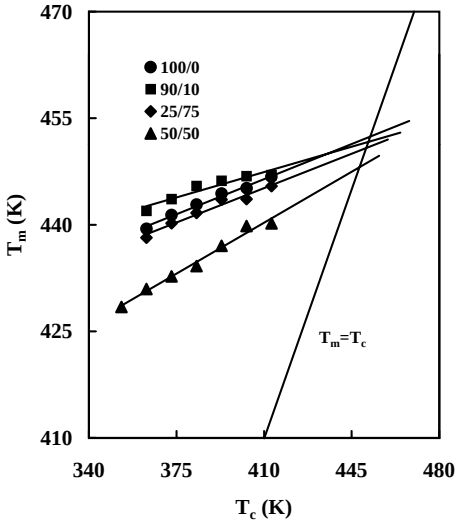

Fig. 7. Hoffman–Weeks plot for PHB/PECH–EO blends.

where T^0_{mb} and T^0_m are the equilibrium melting points of the semicrystalline polymer in the blend and in the pure state, respectively, ΔH^0 is the enthalpy of fusion of the semicrystalline polymer, V_1 and V_2 are the molar volumes of the repeat units in the amorphous and crystalline polymers, respectively, and ϕ_1 is the volume fraction of the amorphous polymer.

For the PHB/PECH–EO blends, using $V_1 = 54.1\ cm^3\ mol^{-1}$ (calculated using $V_{PECH} = 68.03\ cm^3\ mol^{-1}$ [33] and $V_{PEO} = 38.9\ cm^3\ mol^{-1}$ [32]), $V_2 = 75\ cm^3\ mol^{-1}$, $\Delta H^0 = 1.25 \times 10^4\ J\ mol^{-1}$ [14], a negative value $\chi_{PHB/PECH-EO} = -0.089$ is obtained from the slope of the straight line in Fig. 9. The interaction energy density of the polymer–polymer pair, B, is $-6.2\ J\ cm^{-3}$, about half of that of the PHB/PECH blend system [26].

The positive intercept in the Nishi–Wang plot has been explained by a composition dependent χ_{12}. Both $\chi_{PHB/PECH}$ and $\chi_{PHB/PEO}$ are markedly composition-dependent as determined by the depression of the equilibrium melting point of PHB [14,23]. Similarly, a small intercept is obtained for the PHB/PECH–EO blends as shown in Fig. 9, suggesting that $\chi_{PHB/PECH-EO}$ also varies with the blend composition.

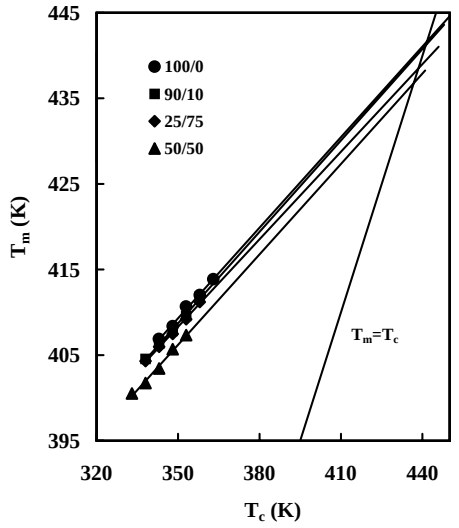

Fig. 8. Hoffman–Weeks plot for PHBV/PECH–EO blends.

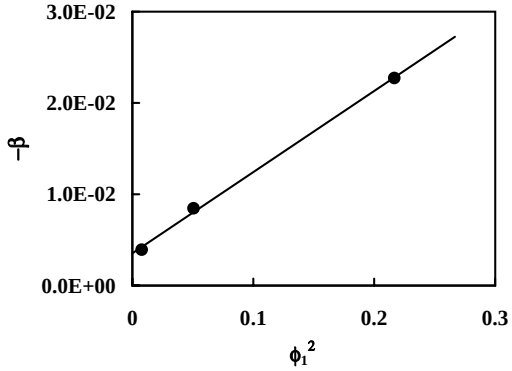

Fig. 9. Nishi–Wang plot for PHB/PECH–EO blends.

As for the PHBV/PECH–EO blends, $\Delta H^0 = 109\ J\ g^{-1}$ [38] and $V_2 = 76.6\ cm^3\ mol^{-1}$ (calculated using $V_{PHB} = 75\ cm^3\ mol^{-1}$ [14] and $V_{PHV} = 86.3\ cm^3\ mol^{-1}$ [41]). A negative value $\chi_{PHB/PECH-EO} = -0.075$ is obtained from Fig. 10, which is consistent with a miscible blend system. As compared to a slightly more negative interaction parameter for the PHB/PECH–EO blend system, it seems that the interaction between PHB and PECH–EO is interfered by the presence of 3HV units. The positive intercept and the relatively poor linear relationship between $-\beta$ and ϕ_1^2 in Fig. 10 strongly suggest that the χ_{12} value of PHBV/PECH–EO blend system is composition-dependent.

3.4. Crystallization behavior

PHB can crystallize from the melt during DSC cooling run at a slow cooling rate (for example 20°C min^{-1}), and thus the glass transition and cold crystallization of pure PHB were not observed in the following DSC heating run. For the quenched samples, cold crystallization peaks were found after the glass transitions of PHB for both pure PHB and

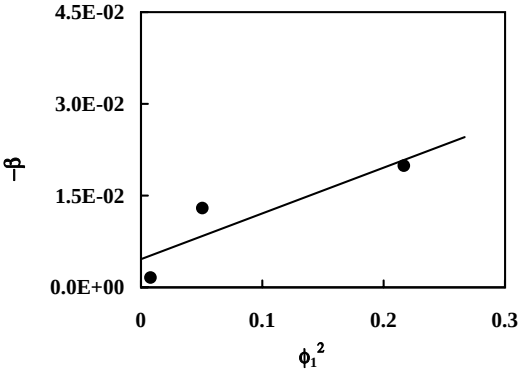

Fig. 10. Nishi–Wang plot for PHBV/PECH–EO blends.

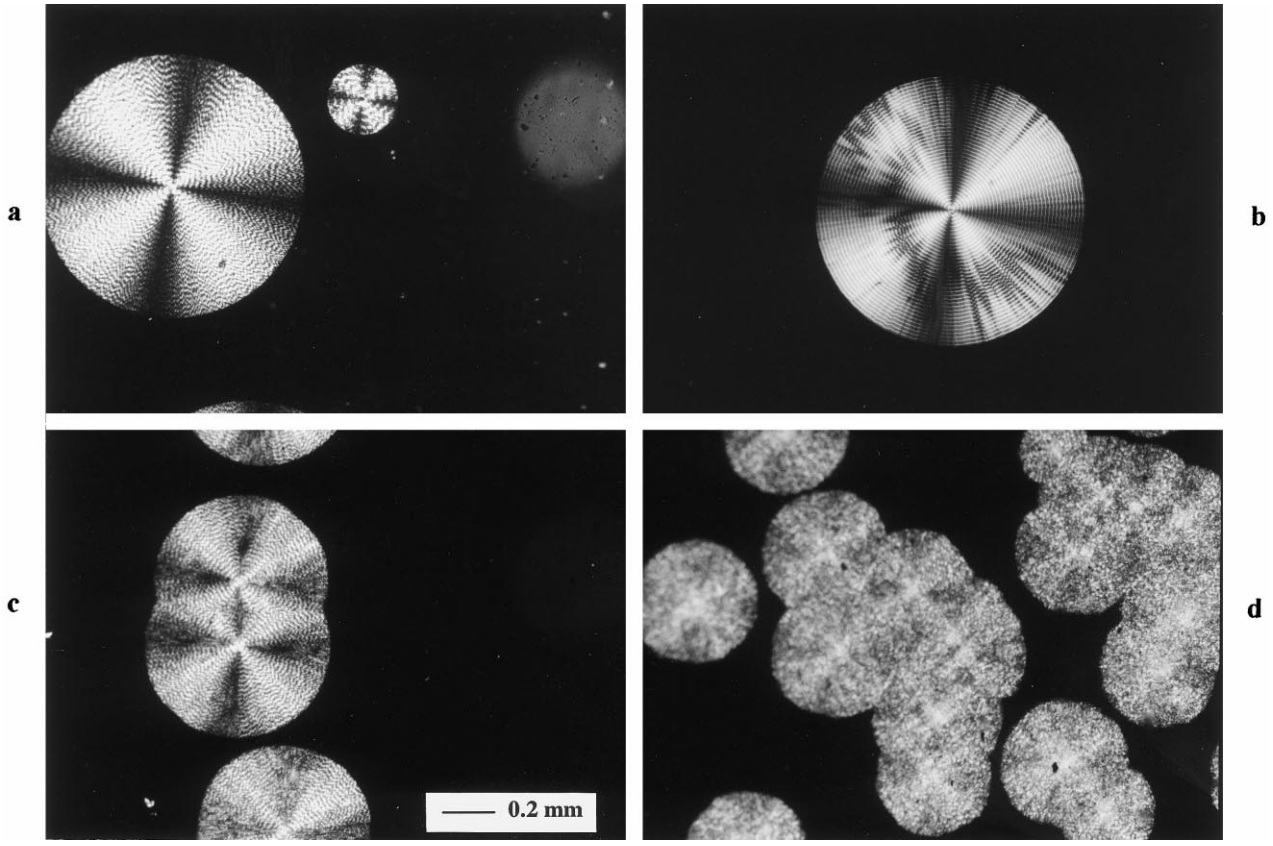

Fig. 11. Polarizing optical micrographs of PHB/PECH–EO blends crystallized isothermally at 90°C (same magnification, bar = 0.2 mm): (a) PHB; (b) 90/10; (c) 75/25 and (d) 50/50.

blend samples during the following heating run (Fig. 1). The cold crystallization temperature (T_{cc}) shows a slight decrease with increasing PECH–EO content from 0 to 50 wt.%, and then a marked increase with increasing PECH–EO content from 50 to 90 wt.% as compared to that of pure PHB (Fig. 3). The result indicates that the addition of PECH–EO may have some positive effects on crystallization of PHB when PECH–EO content is lower.

As shown in Table 1, the enthalpy of cold crystallization (ΔH_{cc}) of pure PHB (absolute value) is much smaller than those in the blends with 25 to 50 wt.% PECH–EO content, implying that the crystallization of pure PHB is very fast. A notable fraction of PHB has already crystallized during the melt quenching process, and consequently the pure PHB sample shows a smaller ΔH_{cc}. It is noted that the ΔH_{cc} of PHB in the PHB/PECH–EO 90/10 blend is even smaller than that of pure PHB mainly because a larger amount of PHB in the blend has crystallized during the melt quenching, indicating a fast crystallization process for this blend. Since crystallization was sufficiently rapid during quenching from the melt, crystalline PHB phase may co-exist with amorphous PHB (for pure PHB) or amorphous blends. This can also be concluded from the large difference between the absolute values of ΔH_f and ΔH_{cc} for quenched samples as shown in Table 1.

For the PHBV/PECH–EO blends, cold crystallization peaks are also found for the quenched samples during the DSC heating runs. The absolute values of ΔH_{cc} and ΔH_f for quenched samples after cold crystallization are close to each other (Table 2), indicating that a large amount of amorphous PHBV exists in the quenched samples of pure PHBV and the blends as a result of slow crystallization of PHBV. PHBV has a lower T_g but a higher T_{cc} than PHB, indicating that it is more difficult to crystallize. This is also supported by the lower spherulitic growth rate (G) of PHBV as discussed below. The T_{cc} increases from 73°C for pure PHBV to 89°C for the 25/75 blend (Fig. 4). The cold crystallization peak is not detectable for the 10/90 blend. The results suggest that the cold crystallization of PHBV is markedly influenced by the addition of the PECH–EO component. As a result, the absolute values of ΔH_{cc} in PHBV/PECH–EO blends are smaller than that of pure PHBV, and hence a significantly lowered Cr value of PHBV observed in the blends as shown in Table 2.

The crystallization of PHB and PHBV from the melt state was studied under isothermal condition at various crystallization temperatures (T_cs). Typical spherulitic textures for various samples crystallized at different T_cs are shown in Figs. 11–13. Volume-filling spherulites were observed in both blend systems at all compositions investigated (0–50 wt.% PECH–EO) when the samples were allowed to crystallize at a suitable temperature for a sufficient period.

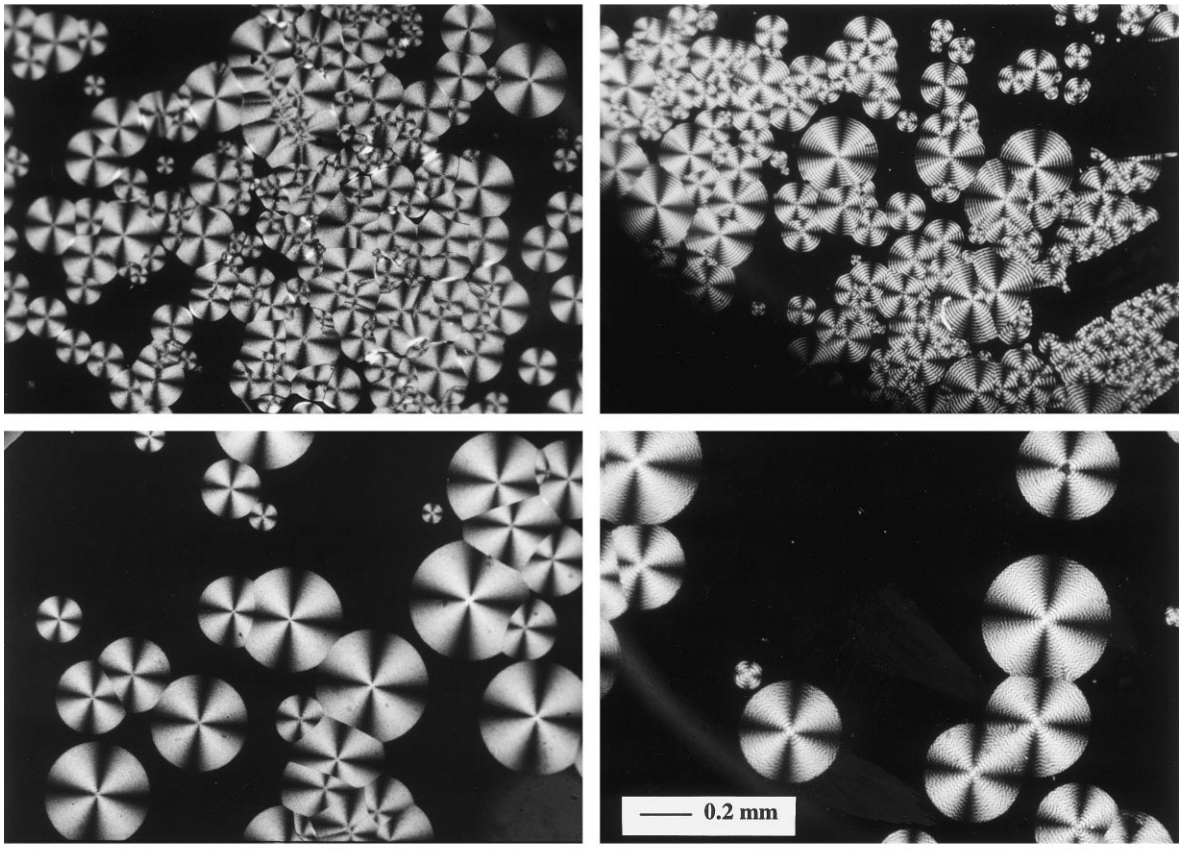

Fig. 12. Polarizing optical micrographs of PHB/PECH–EO blends crystallized isothermally at 60°C (upper) and 70°C (lower) (same magnification, bar = 0.2 mm): (a) PHB and (b) 90/10.

Furthermore, the spherulite radius, R, increases linearly with time until impingement takes place, and no phase separation could be detected as indicated by no rejection of PECH–EO into the interspherulitic regions and in the intraspherulitic zones. The uncrystallizable PECH–EO component is incorporated in the interlamellar or interfibrillar regions of the PHB or PHBV spherulites.

3.5. Spherulitic growth kinetics

Figs. 14 and 15 show the relationships between G and T_c for the two blend systems. The addition of PECH–EO diminishes the maximum values of G (G_{max}) of PHB and PHBV spherulites. There is a gradual shift in temperature of peak growth rate (T_{max}) towards lower T_cs as PECH–EO is added. The shift in T_{max} is well explained by the changes in T_m and T_g as observed in other blend systems [42,43]. The G values of PHB spherulites in the blends are smaller than that in pure PHB at most crystallization temperatures, and slightly higher at 60°C. Similar results are found in PHBV/PECH–EO blends (Fig. 15). The G value of PHBV in PHBV/PECH–EO 90/10 blend is higher than that of pure PHBV when crystallized at 50°C. However, the G value of PHBV decreases with increasing PECH–EO content at T_c above 50°C. An attempt to study the growth of PHB and PHBV spherulites at even lower T_c failed because of dense nucleation.

In general, there are two main factors that can contribute to the depression of crystallization rate in miscible semicrystalline/amorphous polymer blends: a dilution effect which diminishes the formation of a critical nucleus on the front of the growing spherulites, and a decrease in undercooling due to the melting point depression. Apart from these, G is also markedly dependent on the segmental mobility of the semicrystalline polymer molecules which is related to the T_g of the blends. At a lower T_c, since the nucleation is fast, this factor may play an important role in the spherulitic growth. In this case, the lower T_g of the blend makes PHB or PHBV chains move more easily. Thus an increase in G value is observed for PHB/PECH–EO and PHBV/PECH–EO blends crystallized at 60 and 50°C, respectively.

Spherulitic growth kinetics can be analyzed using the Lauritzen–Hoffman theory [44]. According to this theory, the linear growth rate G is expressed as follows:

$$G = G_0 \exp\left(\frac{-U^*}{R(T_c - T_\infty)}\right)\exp\left(\frac{-K_g}{fT_c\Delta T}\right) \quad (9)$$

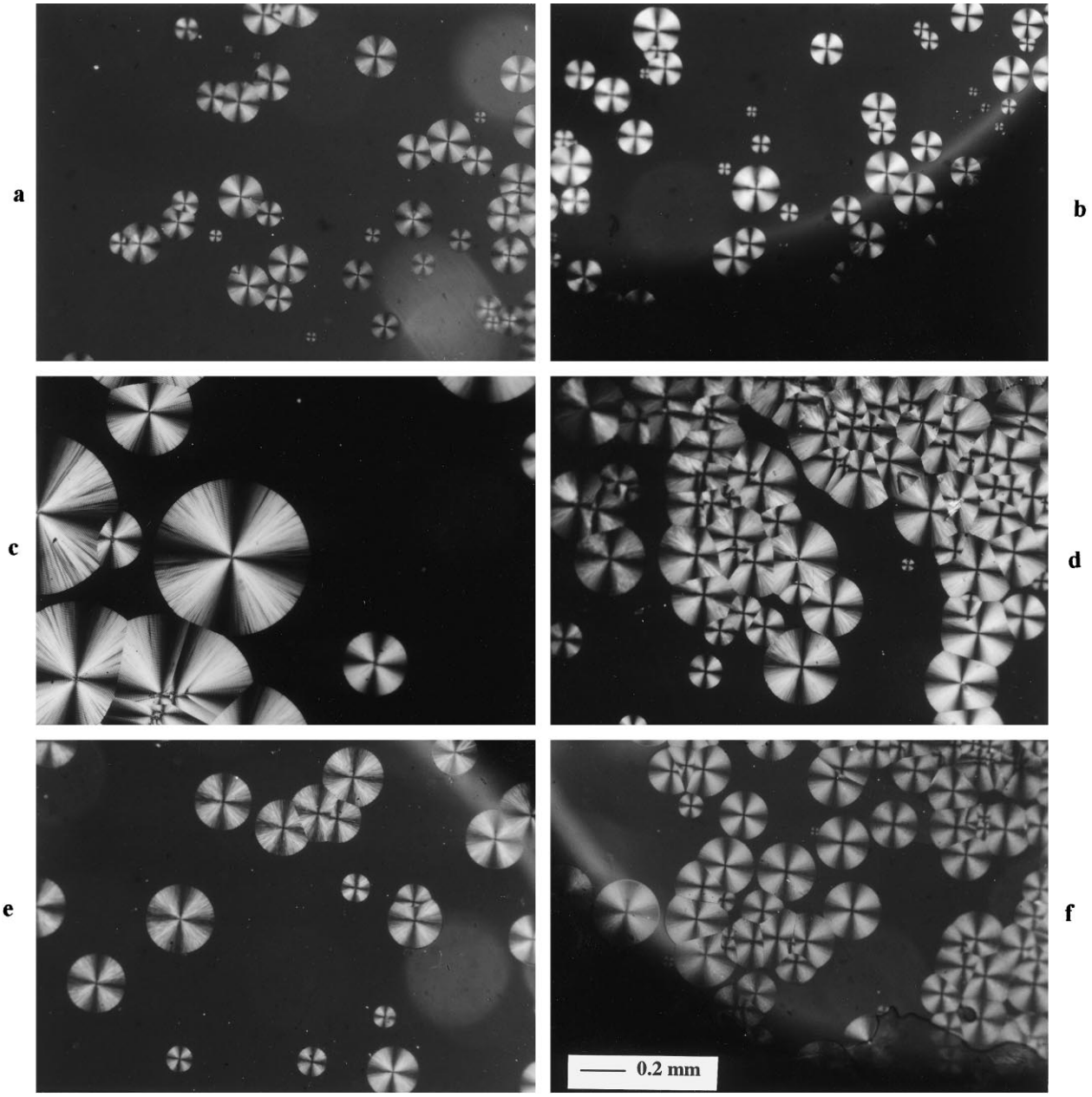

Fig. 13. Polarizing optical micrographs of PHBV/PECH–EO blends crystallized isothermally at 50°C (upper) and 60°C (median and lower) (same magnification, bar = 0.2 mm): (a) and (c) PHBV; (b) and (d) 90/10; (e) 75/25 and (f) 50/50.

where the pre-exponential factor G_0 is temperature-independent, U^* is the activation energy for transport of crystallizable segments to the crystallization front, T_∞ is the temperature below which such motions cease, T_c is the crystallization temperature, $\Delta T = T_m^0 - T_c$ is the degree of undercooling, and T_m^0 is the equilibrium melting point. The factor f accounts for the variation in the enthalpy of fusion ΔH_f with temperature and is given by $f = 2T_c/(T_m^0 + T_c)$. The nucleation constant K_g is expressed by [44]:

$$K_g = \frac{nb_0\sigma\sigma_e T_m^0}{\Delta H_f k} \quad (10)$$

where σ and σ_e are the lateral and end-surface free energies, respectively, of the growing crystal, b_0 is the molecular thickness and k is the Boltzmann constant. The value of n may be 2 or 4, depending on the regime of crystallization which is determined by the relative rates of formation and spreading of new secondary nuclei at the growth front. At sufficiently high undercoolings, regime III may occur, then n is equal to 4 [45].

From Eq. (9), the lower the T_m^0, the lower the degree of undercooling is, resulting in a lower G. The lower the T_g, the lower the T_∞ is. At a lower T_c, the value of $T_c - T_\infty$ is determined mainly by the T_g, hence a higher G is found for PHB blends at $T_c = 60$°C and PHBV blends at

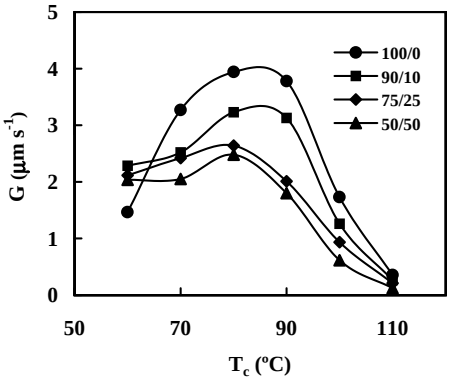

Fig. 14. Radial growth rate (G) of PHB spherulites at various crystallization temperatures (T_cs) for pure PHB and PHB/PECH–EO blends.

$T_c = 50$°C. The data shown in the growth curves for PHB and PHBV blends at different T_cs in Figs. 14 and 15 were used to fit Eq. (9), which can be rearranged to

$$\ln G + \frac{U^*}{R(T_c - T_\infty)} = \ln G_0 - \frac{K_g}{fT_c\Delta T}. \quad (11)$$

The Williams–Landel–Ferry (WLF) [46] values $U^* = 17221.6$ J mol^{-1} and $T_\infty = T_g - 51.6$ K were adopted in our analysis. Using the equilibrium melting point data of PHB obtained from Fig. 7, very good linear relationships between $\ln G + U^*/R(T_c - T_\infty)$ and $1/(fT_c\Delta T)$ were obtained with correlation coefficients better than 0.99 for both pure PHB and the blends (Fig. 16). K_g and G_0 were obtained from the slope and intercept, respectively. Both K_g and G_0 decrease with increasing PECH–EO content in the blends (Table 3). Same treatment has been applied to the spherulitic growth of PHBV/PECH–EO blend system using the data in Fig. 15 and the equilibrium melting point data determined by Fig. 8. Again good linear relationships between $\ln G + U^*/R(T_c - T_\infty)$ and $1/(fT_c\Delta T)$ were obtained (Fig. 17). Similar to the PHB/PECH–EO blends, K_g and G_0 in PHBV blends also decrease with increasing PECH–EO content (Table 3).

Moreover, using the empirical relation [47] $\sigma = \alpha\Delta H_f(a_0b_0)^{1/2}$ and Eq. (10), σ_e can be calculated.

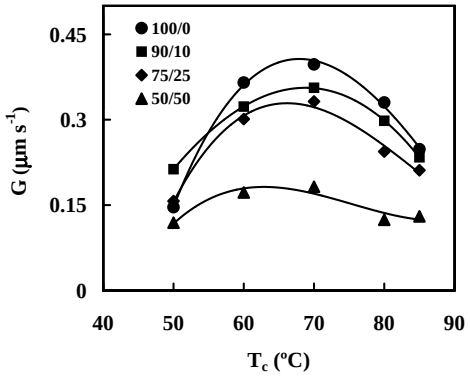

Fig. 15. Radial growth rate (G) of PHBV spherulites at various crystallization temperatures (T_cs) for pure PHBV and PHBV/PECH–EO blends.

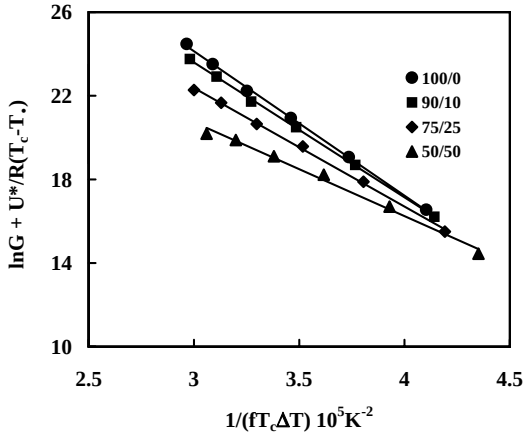

Fig. 16. Lauritzen–Hoffman plot for PHB/PECH–EO blends.

Taking $\alpha = 0.25$ for high-melting polyesters, and using literature values of $a_0 = 6.6$ Å, $b_0 = 5.8$ Å and $\Delta H_f = 1.85 \times 10^8$ J m^{-3} [34], we obtain $\sigma = 28.6 \times 10^{-3}$ J m^{-2}. Hence, σ_e is 58.7×10^{-3} J m^{-2} for pure PHB. This value agrees fairly well with a previously reported value of 46×10^{-3} J m^{-2} [27]. The results in Table 3 show that the end-surface free energy (σ_e) decreases with increasing PECH–EO content in the PHB/PECH–EO blends. It has been suggested that the work of chain-folding q given by $q = 2a_0b_0\sigma_e$ is closely related to chain structure and q is approximately proportional to chain stiffness [44]. The higher the PECH–EO content, the lower σ_e and then the smaller q are. The smaller q value indicates more flexible chains of PHB in the blends. This agrees well with the T_g results from DSC study.

4. Conclusions

Binary blends of PHB/PECH–EO and PHBV/PECH–EO are miscible over the whole composition range. The T_g behavior of both blend systems can be described by the Kwei equation. Negative interaction parameters are

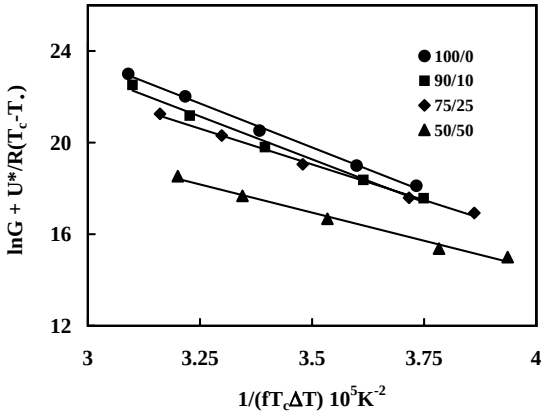

Fig. 17. Lauritzen–Hoffman plot for PHBV/PECH–EO blends.

Table 3
Spherulitic growth kinetic parameters for PHB/PECH–EO and PHBV/PECH–EO blends

Sample	PHB/PECH–EO				PHBV/PECH–EO		
	G_0 ($\mu m\ s^{-1}$)	K_g ($10^5\ K^2$)	R^{2a}	σ_e ($10^{-3}\ J\ m^{-2}$)	G_0 ($\mu m\ s^{-1}$)	K_g ($10^5\ K^2$)	R^{2a}
100/0	4.94E + 17	6.90	0.999	58.7	3.04E + 18	7.67	0.997
90/10	7.50E + 16	6.45	0.999	55.0	9.51E + 17	7.49	0.989
75/25	2.13E + 15	5.67	0.998	48.4	2.13E + 15	6.24	0.996
50/50	1.19E + 13	4.49	0.991	38.6	1.12E + 13	4.91	0.989

[a] Correlation coefficient.

obtained from melting point depression data. Crystallization of bacterial polyesters both from the melt and the glassy state is affected by the addition of PECH–EO. The phase crystallinity of PHB remains unchanged in the cast blends and the samples after cold crystallization. The T_{cc}s of PHB in the blends are lower than that of pure PHB at lower PECH–EO content, and are higher than that of pure PHB at higher PECH–EO content. The phase crystallinity of PHBV shows a slight decrease in the cast blends while it decreases markedly in the samples after cold crystallization. The T_{cc}s of PHBV increases with increasing PECH–EO content in the blends. During isothermal crystallization, the maximum values of G of PHB and PHBV decrease significantly as PECH–EO is added. The radial growth rates of PHB and PHBV spherulites are delayed by PECH–EO at higher T_c. The nucleation constants decrease with increasing PECH–EO content in both blend systems.

Acknowledgements

The authors are grateful to the National University of Singapore for financial support of this work.

References

[1] Poirier Y, Nawrath C, Somerville C. Biotechnol 1995;13:142.
[2] Cox MK. In: Doi Y, Fukuda K, editors. Studies in polymer science: 12. Biodegradable plastics and polymers. Amsterdam: Elsevier, 1994. p. 120–35.
[3] Müller HM, Seebach D. Angew Chem Int Ed Engl 1993;32:477.
[4] Poirier Y, Dennis DE, Nawrath C, Somerville C. Adv Mater 1993;5:30.
[5] Barham PJ. In: Dawes EA, editor. Novel biodegradable microbial polymers, NATO ASI Series, Dordrecht: Kluwer, 1990. p. 81–96.
[6] Steinbüchel A. In: Byrom D, editor. Biomaterials—novel materials from biological sources. New York: Stockton Press, 1991. p. 123– 213.
[7] Doi Y. Microbial polyesters. New York: VCH, 1990.
[8] Anderson AJ, Dawes EA. Microbiol Rev 1990;54:450.
[9] Holmes PA. Phys Technol 1985;16:32.
[10] Hocking PJ, Marchessault RH. In: Griffin GJL, editor. Chemistry and technology of biodegradable polymers. London: Chapman & Hall, 1994. p. 48–96.
[11] Byrom D. Trends Biotechnol 1987;5:246.
[12] Sharma R, Ray AR. J Macromol Sci—Rev Macromol Chem Phys 1995;C35:327.
[13] Verhoogt H, Ramsay BA, Favis BD. Polymer 1994;35:5155.
[14] Avella M, Martuscelli E. Polymer 1988;29:1731.
[15] Lee JC, Nakajima K, Ikehara T, Nishi T. J Polym Sci Part B: Polym Phys 1997;35:2645.
[16] Xing P, Dong L, An Y, Feng Z, Avella M, Martuscelli E. Macromolecules 1997;30:2726.
[17] Xing P, Dong L, Feng Z, Feng H. Eur Polym J 1998;34:1207.
[18] Greco P, Martuscelli E. Polymer 1989;30:1475.
[19] Abbate M, Martuscelli E, Ragosta G, Scarinzi G. J Mater Sci 1991;26:1119.
[20] Yoon JS, Oh SH, Kim MN. Polymer 1998;39:2479.
[21] Gassner F, Owen AJ. Polymer 1992;33:2508.
[22] Hwang SH, Jung JC, Lee SW. Eur Polym J 1998;34:949.
[23] Dubini Paglia E, Beltrame PL, Canetti M, Seves A, Marcandalli B, Martuscelli E. Polymer 1993;34:996.
[24] Sadocco P, Canetti M, Seves A, Martuscelli E. Polymer 1993;34:3368.
[25] Sadocco P, Bulli C, Elegir G, Seves A, Martuscelli E. Macromol Chem 1993;194:2675.
[26] Finelli L, Sarti B, Scandola M. J Macromol Sci—Pure Appl Chem 1997;A34:13.
[27] Pearce R, Brown GR, Marchessault RH. Polymer 1994;35:3984.
[28] Kwei TK. J Polym Sci: Polym Lett 1984;22:307.
[29] Flory PJ. Principles of polymer chemistry. Ithaca, NY: Cornell University Press, 1953, Chapter 12.
[30] ten Brinke G, Karasz FE, MacKnight WJ. Macromolecules 1983;16:1827.
[31] Paul DR, Barlow JW. Polymer 1984;25:487.
[32] Min KE, Chiou JS, Barlow JW, Paul DR. Polymer 1987;28:1721.
[33] Fernandes AC, Barlow JW, Paul DR. J Appl Polym Sci 1984;29:1971.
[34] Barham PJ, Keller A, Otun EL, Holmes PA. J Mater Sci 1984;19:2781.
[35] Arakawa T, Nagatoshi F, Arai N. J Polym Sci: Polym Phys 1969;7:1461.
[36] Pearce R, Marchessault RH. Polymer 1994;35:3990.
[37] Mitomo H, Barham PJ, Keller A. Polym J 1987;19:1241.
[38] Scandola M, Focarete ML, Adamus G, Sikorska W, Baranowska I, Swierczek S, Gnatowski M, Kowalczuk M, Jedliñski Z. Macromolecules 1997;30:2568.
[39] Hoffman JD, Weeks JJ. J Res Natl Bur Std 1962;66A:13.
[40] Nishi T, Wang TT. Macromolecules 1975;8:909.
[41] Graf JF, Coleman MM, Painter PC. The MG&PC Software, V1.1. Technomic Publishing: Lancaster, 1991.
[42] Pearce R, Marchessault RH. Macromolecules 1994;27:3869.
[43] Abe H, Doi Y, Satkowski MM, Noda I. In: Doi Y, Fukuda K, editors. Studies in polymer science: 12. Biodegradable plastics and polymers. Amsterdam: Elsevier, 1994. p. 591–5.
[44] Hoffman JD, Davies GT, Lauritzen Jr. JI. In: Hannay NB, editor. Treatise on solid state chemistry, vol. 3. New York: Plenum Press, 1976. p. 497.
[45] Hoffman JD. Polymer 1983;24:3.
[46] Williams ML, Landel RF, Ferry JD. J Am Chem Soc 1955;77:3701.
[47] Lauritzen Jr JI, Hoffman JD. J Appl Phys 1973;44:4340.